

## Article

# An Innovative System for the Treatment of Rising Dampness in Buildings Located in Cold Climates

Geoffrey Promis <sup>1</sup>, Omar Douzane <sup>1</sup>, Daniel R. Rousse <sup>2,\*</sup> and Thierry Langlet <sup>1</sup>

<sup>1</sup> Innovative Technologies Laboratory (LTI), University of Picardie Jules Verne, Avenue du Thil-Le Bailly, CEDEX 2, 80025 Amiens, France; geoffrey.promis@u-picardie.fr (G.P.); omar.douzane@u-picardie.fr (O.D.); thierry.langlet@u-picardie.fr (T.L.)

<sup>2</sup> Groupe de Recherche Industrielle en Technologies de L'énergie et en Efficacité Énergétique (t3e), École de Technologie Supérieure, Université du Québec, 1100, Rue Notre-Dame Ouest, Montréal, QC H3C 1K3, Canada

\* Correspondence: daniel.rousse@etsmtl.ca; Tel.: +1-514-396-8462

**Abstract:** Signs of wetness in housing are a significant obstacle to the renovation and energy rehabilitation of old and energy-intensive heritage buildings, especially in cold climates. Thus, in order to avoid the numerous possibilities of degradation caused by the moisture transfer phenomena in the building envelope, the a disruptive aeraulic process, which focuses on the ventilation of an air gap between the thermal insulation and the wet wall, has been designed and its assessed. This system avoids the presence of liquid water at the wall surface by maintaining the hygrothermal balance within the wet wall. This enables the mechanical durability of the supporting structure, the absence of biological activity and/or frost and, hence, the durability of the thermal insulation. These issues are investigated through a case study based on a real site. Over a year of measurements, the wet wall was constantly maintained in hygroscopic balance, around 90% RH, guaranteeing the preservation of its mechanical performance, while the insulation layer was kept moisture free. In addition, the proposed model for predicting the appearance and development of biological activity demonstrated its validity, confirming experimental results. These initial results will now lead to the optimization of the aeraulic device, as well as possible use in a summer cooling context to achieve hygrothermal comfort for housing occupants.

**Keywords:** heat and moisture transfer; building materials; rising damp; innovative ventilation system



**Citation:** Promis, G.; Douzane, O.; Rousse, D.R.; Langlet, T. An Innovative System for the Treatment of Rising Dampness in Buildings Located in Cold Climates. *Energies* **2021**, *14*, 3421. <https://doi.org/10.3390/en14123421>

Academic Editor: Fabrizio Ascione

Received: 4 May 2021

Accepted: 26 May 2021

Published: 10 June 2021

**Publisher's Note:** MDPI stays neutral with regard to jurisdictional claims in published maps and institutional affiliations.



**Copyright:** © 2021 by the authors. Licensee MDPI, Basel, Switzerland. This article is an open access article distributed under the terms and conditions of the Creative Commons Attribution (CC BY) license (<https://creativecommons.org/licenses/by/4.0/>).

## 1. Introduction

The current policies that pertain to the energy performance targets for buildings has led to several changes in construction practices, namely by increasing the insulation of the building envelope and improving the airtightness. In old buildings, these changes to the envelope can induce phenomena that did not previously exist, especially those related to humidity: mold development [1,2], deterioration of indoor air quality [3,4] and condensation within the walls, which can lead to a decrease in the durability of the materials [5,6] and their energy performance [7,8]. Therefore, it is now mandatory to evaluate moisture transfers within the building walls, which could become crucial during renovation or rehabilitation projects.

The humidity in buildings is generally a source of structural deterioration, and an unhealthy living environment for housing occupants. The increasing number of chronic respiratory diseases can be explained, among other things, by the state of the indoor environment, with the presence of molds and other microorganisms as the main sources [9]. High humidity plays an important role in the development of these biological pollutants [10]. This gives rise, even today, to many questions about the solutions to be provided, in pal-

liative or curative form (pathology of structures), often at high costs and for which the sustainability is not necessarily guaranteed.

Significant moisture content (especially in the form of water vapor) could be present in a housing structure. Normally, water vapor is eliminated by air exchange, either by a natural air leak through the building envelope, by mass diffusion through the structure or by natural or controlled mechanical ventilation. It can also be removed with classical dehumidification equipment, but residential dehumidifiers have limited ability to remove moisture during winter due to low air temperatures [11]. Thermoelectric coolers and desiccant materials-based systems can also be used, but the humidity transfer rates are generally low [12]. Many current high-humidity and condensation problems in severely moisture-contaminated buildings can be better resolved by controlling moisture sources than by using a dehumidifier or increasing the air exchange rate. Moisture sources can be: (i) rainwater diffusing through roofs and walls; (ii) leaks or bursts of water pipes; (iii) indoor sources such as showers, cooking, washing . . . ; (iv) moisture in the building materials; (v) moisture in the foundation walls; and (vi) rising capillary by mass diffusion through the basement structure [13].

One of the most frequent sources of moisture, and the most difficult to treat, is the rising humidity from undrained soils, commonly known as capillary rise, that occurs by capillary suction, osmotic pressure or electro-osmosis [14]. The water rises through the permeable building materials, progressing until there is a balance between absorption (quantity of entering water) and evaporation of water (quantity of leaving water). This phenomenon is governed by factors such as the amount of water in contact with the building element, the conditions of surface evaporation, porosity, thickness, orientation and the presence of salts [15].

Currently, the solutions used to overcome the humidity source problems consist of creating a physical barrier that limits the progression of the water in the walls: implementation of a waterproof film on the walls, waterproofing of the basement of a building (case capillary lifts) or installation of drains. Alternative solutions have also appeared on the market. Examples of these include resin injection in order to reduce the porosity of the wall, or even the installation of electric polarization devices, which repel water by electrophoresis or electro-osmosis. However, these operations are often complex and costly and are not guaranteed to provide a long-term solution. Indeed, due to the complexity and variability of the factors, the results obtained may be unpredictable and/or unsustainable [14]. Choosing the most appropriate technique must be based on a comprehensive diagnosis of the origin of the problem by studying the expected effectiveness of the solution provided while also keeping in mind the costs involved. Typical techniques for treating rising humidity are based on four intervention principles [14]: (1) preventing water from entering the walls, (2) removing excess water from the walls, (3) preventing rising water in the walls and (4) hiding apparent anomalies. The technical solutions currently implemented on the renovation market require significant work and are therefore, for most of them, very expensive. The most efficient processes can also be difficult to apply, and may only be viable in very specific conditions, all of which require a specialized workforce. In some cases, an intervention may require dramatic physical changes to the building, strongly impacting the architectural aspect of a heritage structure.

Few research works currently focus on these subjects, due to the complexity of the physical problems involved (coupled heat and moisture transfers, aeratics, etc.). Nevertheless, in several European countries, investigations have been carried-out to develop two different solutions: the University of Stockholm is studying the implementation of a ventilated and heated double skin [16–19], and the Laboratory of Building Physics (LFC) of the Porto University of Engineering proposes ventilating only the base of the wet wall [20–25]. These technical solutions involve strengths and weaknesses linked to their mode of operation and regulation, their implementation, their effectiveness or their long-term sustainability: deep changes in the building envelope to create a unique ventilation network for the floors

and walls, installation of a 15 W/m heating cable in permanent operation and intervention on both sides of the wet walls, without any guaranteed long-term results.

In this context, this work presents an experimental campaign carried out on a novel full-scale in situ single operation-based solution to deal with humidity problems in the context of renovations or rehabilitations. The aim of this study is to determine the ability of a genuine dynamic aeraulic system to sanitize the walls by extracting and controlling humidity from the air confined between the support wall and the insulator. The specific objectives can be summarized as follows:

- Ensuring the durability of rehabilitation works carried-out on renovated buildings;
- Preventing the appearance and proliferation of biological activity;
- Maintaining the moisture balance of the wall in its environment;
- Providing a cheap and yet effective solution.

Here, the investigation is limited to pathological mechanisms from capillary rise within the building envelop to ensure the conservation and the durability of historic buildings (and avoiding the deconstruction and inherent environmental impacts) and the durability of the building envelope, materials and their suitability. Lowering the moisture content will have an impact on air quality, but this specific is not addressed quantitatively in the paper. Finally, the complete energy consumption, and therefore yearly operation cost, of the device is not monitored in this first performance assessment.

The preponderant interest of the proposed system is that the ventilation, calibrated according to the moisture content of the air gap, which in turn depends on the water diffusion rates, keeps the insulation linings and facings perfectly healthy. The second interest is that renovations can be undertaken without delay and without preliminary work to dry out the supports.

The exploratory approach proposed here is based on an aeraulic pre-dimensioning of the used ventilation system in order to assess the dynamic and linear aeraulic pressure losses. The system is implemented in the walls of a damp old house during its thermal renovation. An in situ monitoring of the thermo-hygric behavior of the real wall then allows the global efficiency of the sanitation system to be evaluated, and further investigation into the use of this technology for other applications. This first step is the starting point for optimizing the design of the process, based on the knowledge of thermal, hygroscopic and aeraulic interaction phenomena, which will then be reproduced in the laboratory and modeled to propose an efficient and sustainable solution to the problems of moisture infiltration in the walls of buildings.

## 2. Materials and Methods

### 2.1. Principle of the Ventilation System

The proposed technology is a forced-convection aeraulic system for the sustainable energy renovation of old buildings with damp walls. Thin buffer spaces are enabled between each damp wall and its thermal insulation. This creates potential channels to evacuate moisture from the wall before it reaches the insulation layer (Figure 1). Moisture is thus removed from each buffer space by replacing the moist air with fresh air. For this purpose, a fresh-air blowing duct (shown in red in Figure 1) and a wet-air suction duct (schematically depicted in blue in Figure 1) are located in the buffer spaces, each of which involves small apertures properly distributed to provide a uniform flow.

Blowing is carried out with air jets that effectively expel moisture from the bottom of the walls. This wet air removal is performed daily in a uniform manner in each buffer space. Thus, all thermal insulation and siding materials that usually cover the wet walls remain completely protected from moisture, ensuring their durability. As the ventilation system prevents vapor diffusion through the insulation layer, an almost immediate improvement in air quality is perceived and the comfort of the occupants rapidly increases. On the other hand, the “benefits” brought by the presence of moisture in the walls of old buildings are preserved and even valued:

1. Wet walls retain their hygroscopic balance, and their operation is preserved. Specialists in sustainable rehabilitation advocate for letting these walls “breathe” to preserve the integrity of old buildings and thus ensure their sustainability (the drying of some old walls is sometimes detrimental and may even lead to premature collapse).
2. In hot weather, especially during heatwaves, cooling should be ensured in the premises by evaporation of moisture from the walls. The discomfort to occupants, which is usually created by the moisture produced by evaporation and by the direct presence of the cold wall surfaces, should not exist. The effective cooling is of course less than that produced by air conditioning installation, but the energy consumed is negligible with respect to such systems.

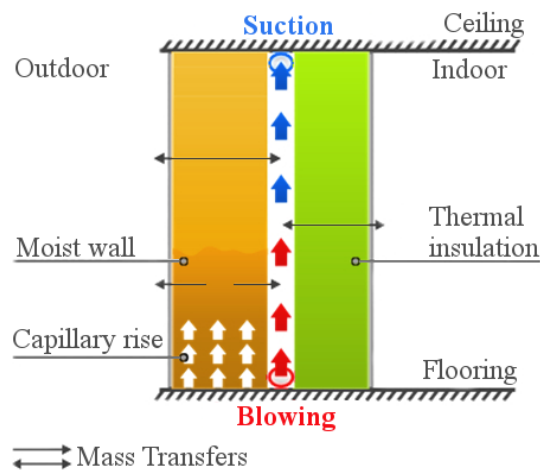


Figure 1. Principle of ventilation technology.

### 2.2. Aeraulic Dimensioning

The removal of moisture between the wall and the thermal insulation is carried out by periodically renewing all humidity-laden air in the buffer space with fresh air taken from outside. This periodic use allows one to avoid continuous operations that would lead to important ventilation costs. Figure 2 schematically depicts the elements of the system installed on a damp wall (1) between the floor (9) and the ceiling (10) of a room to be rehabilitated. The sanitation (buffer) space (7) is located between the surface of the wall and a screen (2) with an appropriately selected water vapor permeability. This screen is covered by a thermal insulation layer (8). In this space (7), an inflow pipe (3) with small blowing apertures (5) is located on the floor, and an outflow pipe (4) with small suction apertures (6) is located right under the ceiling.

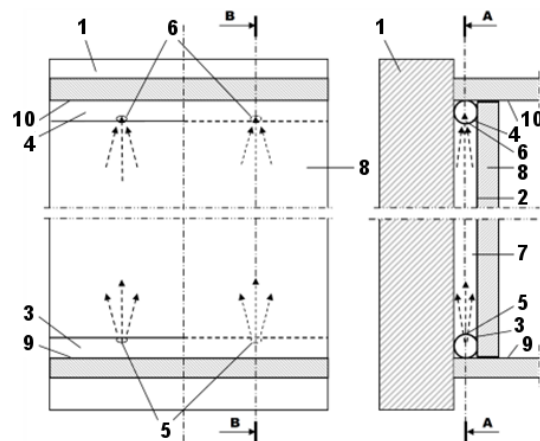


Figure 2. Arrangement of the elements of the blowing and suction system.

The pressure in the blowing line is controlled such that a vertical air jet is created at each blowing aperture. With appropriately distributed jets (5) and suction apertures (6) as shown in Figure 2, the evacuation of moist air is carried out uniformly throughout the sanitation space thanks to two complementary phenomena: the Coanda effect and the induction phenomenon [26].

In order to calculate the blowing and suction networks, the ventilation system proceeds successively with the following calculations:

- Calculation of each perforated pipe of the network carried out “step by step” for each of its segments, taking into consideration the air side pressure losses caused by the blowing and suction networks;

$$\frac{\Delta P_s}{\Delta L} = \frac{\lambda \rho V^2}{2D} \quad (1)$$

- Calculation of the overall aeraulic characteristics of the pipes thanks to series and parallel approaches, in particular the characteristic of the volumetric air flow rate  $Q$  at the inlet as a function of applied input pressure  $P$ :  $Q(P) = gP^h$ ;
- Direct calculation of the whole network flows,  $Q(P)$ , for pressures of 100 Pa and 400 Pa;
- Direct calculation of global characteristics of the whole network  $Pt = aQt^b$ ;
- Establishment of the operating point  $Pt$ , and of the associated volumetric air flow rate  $Qt$  regarding the choice of the fan;
- Direct calculation of the pressure  $P$  and the volumetric air flow rate  $Q$  for each segment regarding operation of the current network;
- “Step-by-step” calculation of blowing and suction air flows with respect to the operation of the current network during sweep scan;
- Determination of the daily sweep time  $D_b$  for the whole network.

This iterative calculation allows the determination of the operating point of the network and provides the appropriate blowing or suction flow rate values for each perforated pipe section, as well as the corresponding sweeping times. The sequence of operations required to calculate a network occurs automatically, according to the nature and configuration of the various perforated pipes in it and based on all the data relating to the constituent perforated pipes and their connection technology.

### 2.3. Experimental Validation

An aeraulic measuring bench was realized to validate the chosen methodology and the calculation of operating point and volumetric air flow rate (Figure 3). This experimental device consists of a fan with adjustable blowing pressure, from 0 to 5 kPa (HELIOS SlimVent SVV80). The flow/pressure torque is controlled by 4 shunt by-pass exhaust valves at the entrance which allow the regulation of the volumetric air flow rate from 0 to 72 m<sup>3</sup>/h. The pressures are measured using 4 water column manometers (500 mm high), and the air flows are measured by 2 genuine custom venturis.

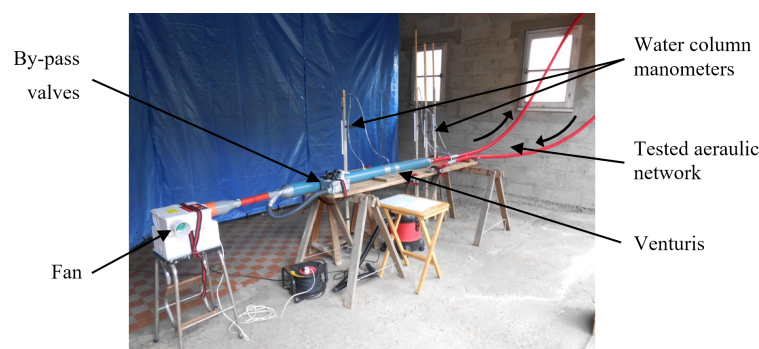


**Figure 3.** Aeraulic apparatus used for the experimental validation for the design methodology.

The characteristic of custom venturis is assessed from blowing tests at different volumetric air flow rates, from 5 to 90 m<sup>3</sup>/h as presented in Figure 4. The volumetric air flow rate vs. differential pressure of venturis is fitted according to the following function, from the principle of energy conservation of Bernoulli's theorem:

$$Q = K \times \sqrt{\Delta P} \quad (2)$$

where  $K$  represents a coefficient taking into account the density and compressibility of the fluid, the coefficients of discharge and approach velocity, gravity and the cross-sections of the venturi. The custom venturis used in the aeraulic apparatus show  $K = 5.20 \pm 0.01 \text{ m}^3/(\text{h} \cdot (\text{mm H}_2\text{O})^{1/2})$ .

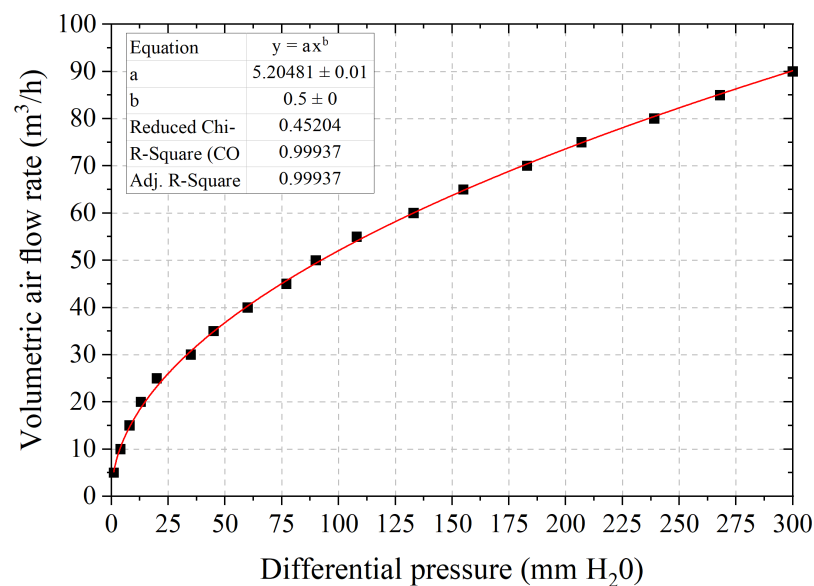


**Figure 4.** Characteristics of the custom venturis expressed as volumetric air flow rate vs. differential pressure.

The measurement of the differential pressure between the inlet and the outlet of the aeraulic network leads to the establishment of the operating point of the experimental device. The measurement precision using water column manometers is 1 mm, which leads to an experimental precision of the network operating point of the order of 10 Pa, and of the volumetric air flow rate of 3.5 m<sup>3</sup>/h.

Tests are carried out on four different aeraulic networks (diameter, internal surface roughness) with different drilling configurations:

- IRL 25 tube unperforated (Length = 1 m, external diameter = 25 mm and internal diameter = 21.7 mm)
- IRL 25 tube with a length of 1.8 m consisting of 30 sections of 6 cm delimited by 5 mm diameter holes.
- TPC 40 unperforated ringed sheath (length = 24 m, external diameter = 40 mm and internal diameter = 32 mm)
- TPC 40 ringed sheath (4.5 m long unperforated followed by 15 m made up of 30 sections of 50 cm delimited by 5 mm diameter holes)

The experimental results are compared with the corresponding results obtained from the analytical approach in Figure 5, where the evolution of the network operating point according to the imposed flow is presented for the four tested configurations. The correlation coefficient ( $R^2$ ) is close to 1 in all four cases, which tends to demonstrate the robustness of the aeraulic approach formulated herein. Nevertheless, results show a small difference between experimental and analytical data in the case of non-perforated TPC40 tubes, for relatively high flow rates, greater than 50 m<sup>3</sup>/h. Although the error is non negligible

(in the order of 10% maximum), the ventilation system used in the case of the sanitation of the walls never reaches these high rates.

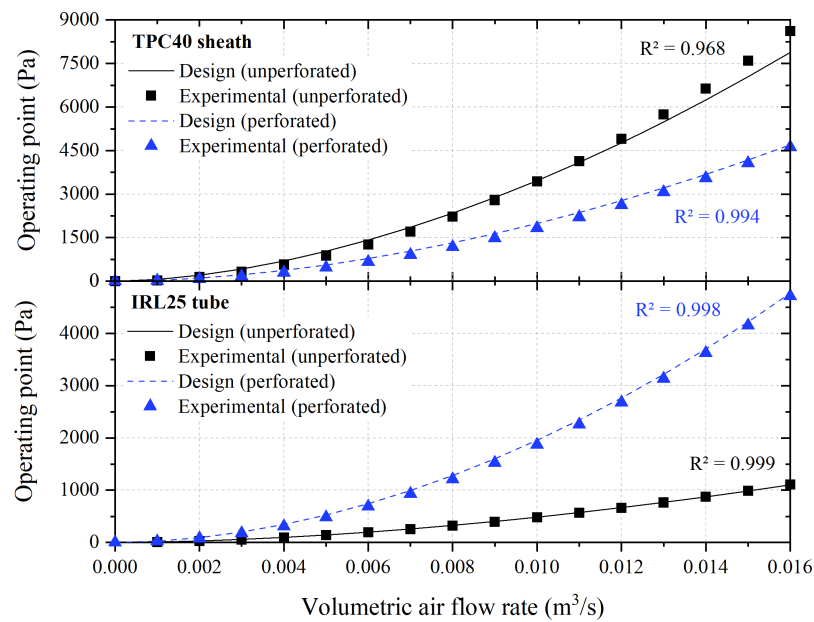


**Figure 5.** Evolution of the network pressure operating point, according to the volumetric air flow rate for the for aeraulic configurations tested.

#### 2.4. Case Study Using the Ventilation Device

After laboratory validation, the experimental device was implemented in a detached old house located in Puiseux-en-Retz in the Picardie region of Northern France. The dwelling equipped with the aeraulic system is a two-floor stone house and comprises two buildings arranged in an L-shape. Semi-buried walls facing south (on the left in Figure 6) are the most affected by water infiltration and risk of frost. The system is implemented on both floors, but only the cellar, on the bottom floor, was subject to hygrothermal monitoring (Figure 6).



**Figure 6.** Building in which the aeraulic device is located.

Figure 7 shows traces of moisture and biological activity visible on the partly-buried stone wall of the cellar. Before renovation, the water beaded directly onto the surface of the wall, forming a thin film of water on the surface; the relative humidity on the inside surface of the wall can therefore be considered equal to 100%. Signs of biological activity are also visible on the surface of the wall, particularly through mold that develops in this environment (mild temperature and liquid water).



**Figure 7.** Moist wall with development of the biological activity.

The thermal renovation project consists of the installation of a 6 cm fibrous insulation with 13 mm plasterboard interior panelling. The ventilation of the air gap between the supporting structure and the thermal insulation was carried out by means of PVC perforated tubes (PVC DN40, internal diameter of 34 mm) located at the top and at the bottom of the wall. With calculations carried out with the above-mentioned methodology, the average blowing and suction volumetric air flow rates for each aperture is  $0.00018 \text{ m}^3/\text{s}$ , which leads to an operating pressure of around 286 Pa. A ventilation period of 30 min of operation per day is required in order to carry out 4 air exchanges each day. Hence, the energy requirement for the system remains quite negligible for the whole year at 6.3 kWh yearly. All relevant calculation results are summarized in Table 1.

**Table 1.** Specifications of the aeraulic device.

	Blowing	Suction
Ducts		PVC DN 40
- Length (m)	25.5	25.5
- Internal diameter (mm)	34	34
- Spacing between holes (cm)	50	50
- Hole diameter (mm)	5	5
- Average air flow rate ( $\text{m}^3/\text{h}$ )	0.65	0.65
Fans		SlimVent SVV80 (HELIOS)
- Operating pressure (Pa)	286	286
- Volumetric air flow rate ( $\text{m}^3/\text{h}$ )	33	33
- Operating time (min/day)	30	30
- Consumed energy (kWh/scan)	0.017	0.017
- Consumed energy (kWh/year)	6.3	6.3

Figure 8 shows the installation of the blowing and suction piping. In order to avoid dust in the air gap and ensure durability, an HPV screen (High Water Vapor Permeability flexible screen) is also installed between the air gap and the insulation layer. Finally, a structure composed of metal rails is used to fix the thermal insulation and to support the plasterboard interior paneling.

The overall cost of the whole system is 250 euros, excluding insulation and insulation structure. The annual energy cost for the ventilation system is below one euro, while the extra heat cost, based on the expelled mass flow rate, induced by the half-hour daily operation is less than 20 euros per year, making this solution affordable. Maintenance costs (cleaning or replacement of the filter) after about 180 h of yearly operation have not been accounted for in the preliminary work.

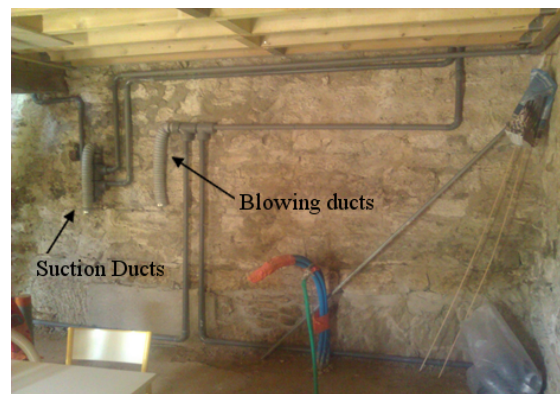


Figure 8. Instrumentation of a semi-buried wet wall.

The buried wall of the cellar was instrumented with different calibrated temperature (T-type thermocouples) and relative humidity (VAISALA HMP60) probes. The latter were arranged at various heights and depths in the wet wall and in the ventilated air space, as presented in Figure 9. Additional probes were installed inside the cellar and outside the house (sensors 1 and 8). Temperature sensors were located on the surface of the stone wall and on the interior finishing plasterboard (respectively  $T_{smi}$  and  $T_{si}$ ). The sensors were connected to a Graphtec GL 800 mini data logger. Data recording followed a frequency of  $1.67 \times 10^{-3}$  Hz. Data acquisition was carried out over a period of more than a year.

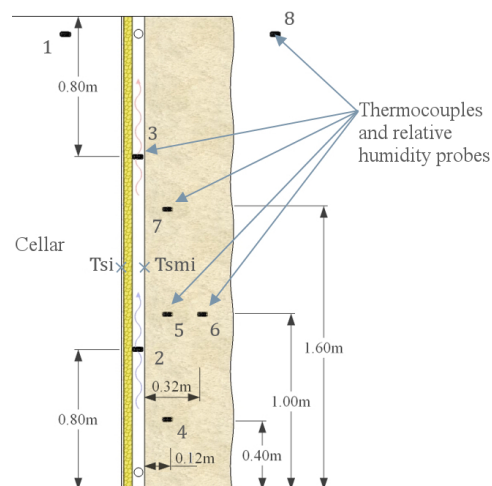


Figure 9. Schematic of the installation of the aeraulic dehumidifying system.

### 3. Results and Discussion

#### 3.1. Outdoor Climate and Indoor Ambiance

Figure 10 presents changes in indoor and outdoor relative humidity and temperature over the entire measurement period. In summer (left part of Figure 10), the temperature varied between 10 °C and 30 °C, while the relative humidity fluctuated between 40% and 80%. In winter, the temperature and relative humidity varied between  $-5$  °C and 10 °C and between 70% and 90%, respectively. This case study was then performed with a temperate climate and significant rainfall. In Figure 10, solid lines show daily mean temperature and relative humidity, indoor (grey) and outdoor (black). The shaded areas represent variations in temperature and relative humidity measured by sensors 1 and 8, which recorded these environmental data with a frequency of 10 min. As expected, these variations were significant outside the building, especially in summer. This can impact the operation of a smart ventilation system, self-regulated by the use of instantaneous environmental data. A regular operation was chosen, independently of the external climate, as specified in Table 1 (30 min per day). During the fall and winter seasons, the relative

humidity reached 90% enabling much mass transfer through the wet wall. In summer, although the relative humidity was lower (around 70%), the high temperature caused a significant increase in the saturated water vapor pressure, resulting in a high water content in the outside air. These conditions can also govern substantial mass transfer by diffusion within the walls.

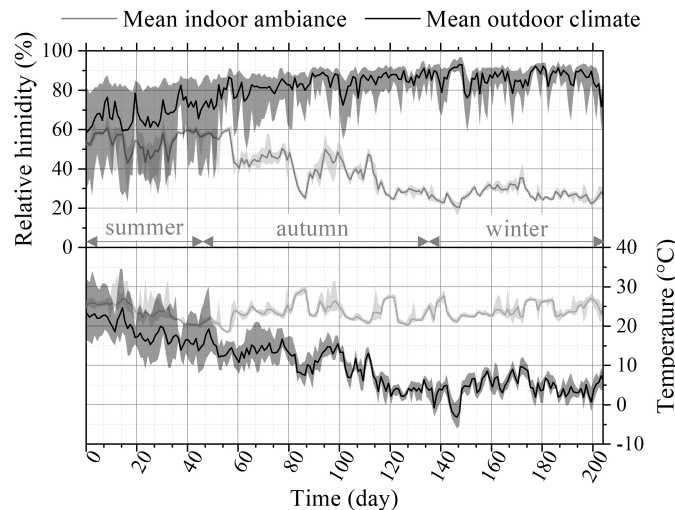


**Figure 10.** Evolution of the outdoor (black) and indoor (grey) relative humidity and temperature. Solid lines represent the daily mean measurements while shaded areas represent variations measured each day by sensors 1 and 8.

Figure 10 shows also the evolution of temperature and relative humidity inside the measurement room (sensor 1 is located in the cellar) where the boiler serving the entire house was installed. The impact of the heating system on the indoor temperatures and relative humidity is not negligible. After installation of the boiler, the indoor temperature remains relatively stable and high (around  $23\text{ °C} \pm 4\text{ °C}$ ). In addition, the relative humidity was low, less than 40%. Relative humidity was strongly influenced by the boiler, which radiates heat and dries the indoor ambiance. This observation is confirmed by the fact that the relative humidity of the cellar increases up to 60%RH in summer, when the boiler is not in use.

### 3.2. Analysis of the Hygrothermal Behavior of the Wall: Efficiency against Water Transfers

First, the temperatures and relative humidities were measured in the wet or damped wall using probes 4 to 7. Probes 4, 5 and 7 were located close to the inner surface, while probe 6 was about 32 cm deep. The initial observations highlighted the presence of liquid water on the inner surface of the wall due to liquid flow transfers within the wet wall, and condensation due to the temperature difference between the heated room and the wet wall. The ventilation system then makes it possible to suppress the presence of liquid water, as can be seen in Figure 11, where relative humidity levels are always well below 100%, regardless of the season. The relative humidity at the core of the wall was higher, above 92%, while the relative humidity at the surface was kept below 90% (probe 7 was damaged during the renovation phase; the data collected are unfortunately not usable). The measured temperatures inside the wall are relatively homogeneous (see Figure 11) and highly dependent on the outside temperature. Thus, the evolution of the relative humidity represents the hygroscopic flows in the wall: an equilibrium appears to have been reached, helping to maintain the mechanical performance and to suppress liquid water on the wall surface. Moisture content is higher during colder periods due to the impact of temperature on the water storage capacity of moist air.

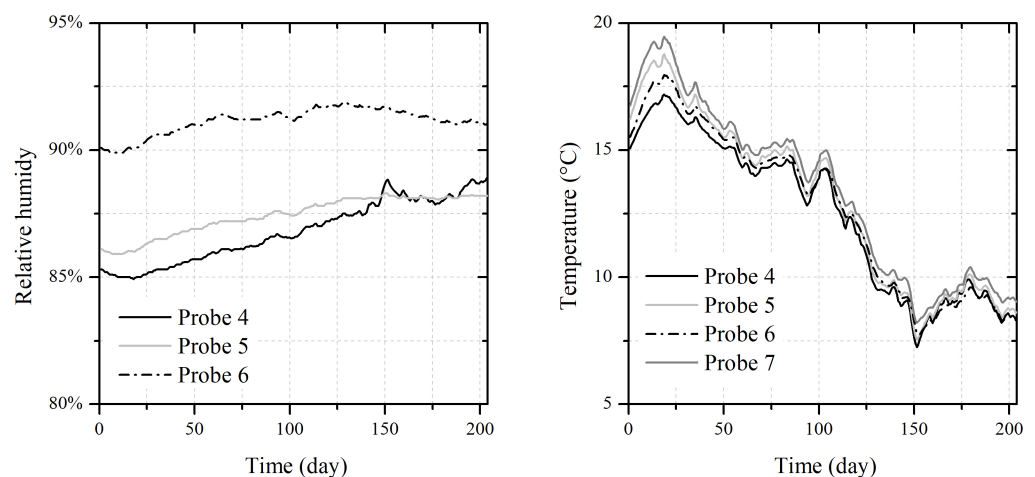


**Figure 11.** Evolution of relative humidity (**left**) and temperature (**right**) in various depths of the wet wall: Probe 4 is placed at the bottom of the wall, probe 5 at 1 m height, probe 6 at 32 cm depth and probe 7 at 1.6 m height.

Probes 2 and 3 made possible to record the changes in temperature and relative humidity in the air gap, in the lower and upper part, respectively. Figure 12 shows a higher relative humidity in the upper part of the air gap. Nevertheless, in view of the significant temperature differences between the top and bottom, it cannot be concluded that the air becomes loaded with moisture as it moves along the wet wall. Indeed, in spite of the fact that the air intake is located on the roof, the ventilation system will generate a heating of the air blown in, as it progresses through the blowing network. The air blown is then a little warmer than the wall, and cools on contact with the cooler surface. The temperature drop will then change the water vapor storage capacity, which explains the increase in relative humidity shown in Figure 12.

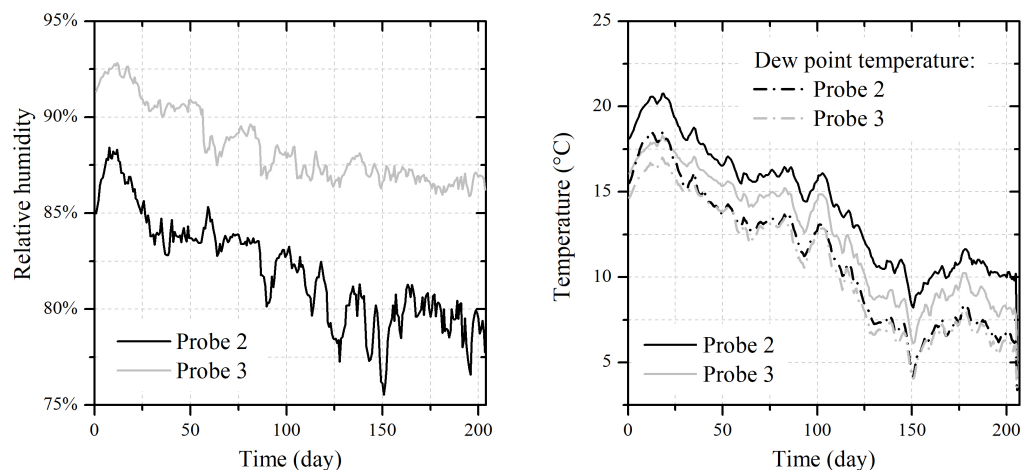


**Figure 12.** Evolution of relative humidity (**left**) and temperature (**right**) in the ventilated air space: Probe 2 was placed at the bottom of the air space while probe 3 was fixed at the top of the air space.

On the other hand, the absence of water vapor condensation in the ventilated air gap is addressed by calculating the dew point temperature, expressed as follows [27]:

$$T_r = \sqrt[3]{\varphi} \cdot [112 + (0.9T)] + (0.1T) - 112 \quad (3)$$

It was found that the temperature in the ventilated air space was always higher than the dew point temperature, both at the top and bottom, thus guaranteeing no condensation. In the lower part, the average difference between the dew point and the measured temperature was about 3 °C, while a difference of 1.9 °C was calculated in the upper

part. The hygrothermal dynamics in the air gap can then be approached by studying the evolution of the absolute humidity  $\varphi^{abs}$  [28]:

$$\varphi^{abs} = \frac{M_w}{M_a} \times \frac{P_v}{P_a} \quad (4)$$

where  $M_w$  and  $M_a$  are the molar mass of water and air, respectively,  $P_v$  the vapor partial pressure and  $P_a$  the dry air pressure.  $P_v$  depends on the vapor saturation pressure  $P_v^{sat}$ :

$$P_v = \varphi \times P_v^{sat}(T) \quad (5)$$

and

$$P_v^{sat}(T) = \exp\left(23.5771 - \frac{4042.9}{T - 37.58}\right) \quad (6)$$

Figure 13 presents the evolution of the absolute humidity with respect to time for probes 2 and 3, respectively. The absolute humidity was higher in summer than in the fall and winter periods, leading to higher moisture transfers during summer. In the case of a semi-buried wall, moisture transfers were horizontal and vertical but capillary rises were stronger during summer, as shown by the significant difference between probes 2 and 3. During this season, a greater amount of water in the lower part of the ventilated air gap was observed, as outside temperatures were at their highest. The air blown from the roof has a high temperature (between 20 °C and 30 °C) and a daily relative humidity of more than 60%. The absolute amount of water present in the air was then significant, greater than that present on the wall surface. The overall system was balanced with water vapor transfers towards the wet wall. Nevertheless, during the summer period, the risk of condensation remained low (see Figure 11). These mechanisms would then limit the temperature rise of the wall and could generate surface cooling, contributing to summer comfort for building occupants. Condensation risks are stronger during winter period, when temperature is low, with a weak moisture holding capacity of air. A refined analysis of the ventilation system impact is thus proposed on the 150th day when a sudden fall of temperature within the air gap is shown.

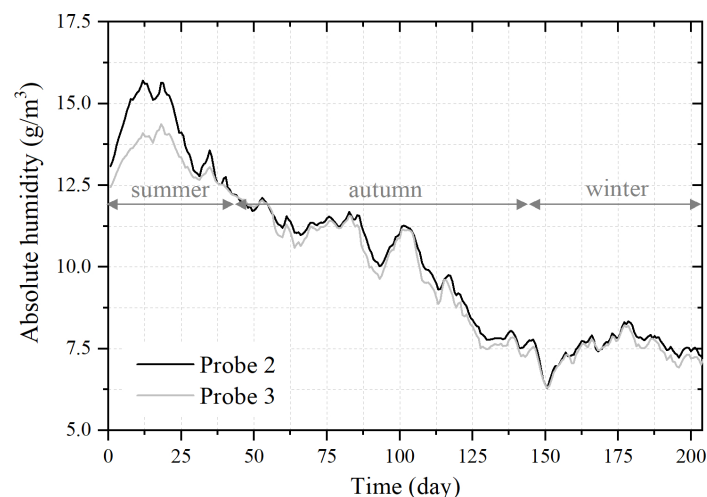


**Figure 13.** Evolution of absolute humidity in the ventilated air space: Probes 2 and 3 are fixed at the bottom and the top of the air space, respectively.

Figure 14 shows the changes in absolute humidity in the wet wall during operation of ventilation device on a much smaller time scale. The absolute humidity content in the wall (probes 4, 5 and 6) was relatively constant, which is a sign of hygroscopic equilibrium. The absolute humidity of the air blown into the air gap also showed very small variations, with a noticeable increase in absolute humidity a few minutes after switching on the aeraulic system, between the 100th and 150th min (probe 2). On the other hand, probe 3

shows a different behavior: before ventilation of the air gap, hygroscopic balance is visible with a relatively stable absolute humidity content, followed by a sudden increase in the absolute humidity content for about 40 min after  $t = 100$  and then a return to equilibrium. An increase in absolute humidity is synonymous with an increase in the amount of water, in the form of vapor, in the ventilated air space. On contact with the wet wall, the air is charged with water molecules, which are then evacuated by the suction system at the top of the wall. This phenomenon shows the dynamics induced by the system that produces a water transfer towards the ventilated air gap. This is caused by the modification of the hygroscopic exchange coefficient at the interface between the wall and the air gap. The forced convection of air will increase this exchange coefficient and thus evacuate the water vapor present on the internal surface of the wall. The absolute humidity within the air gap increases at an average speed of around  $4.86 \text{ g/kg}_{\text{dry air}} \cdot \text{h}$ , thus ensuring the absence of surface condensation. The low ventilation speeds used then govern this low rate of water vapor evacuation.

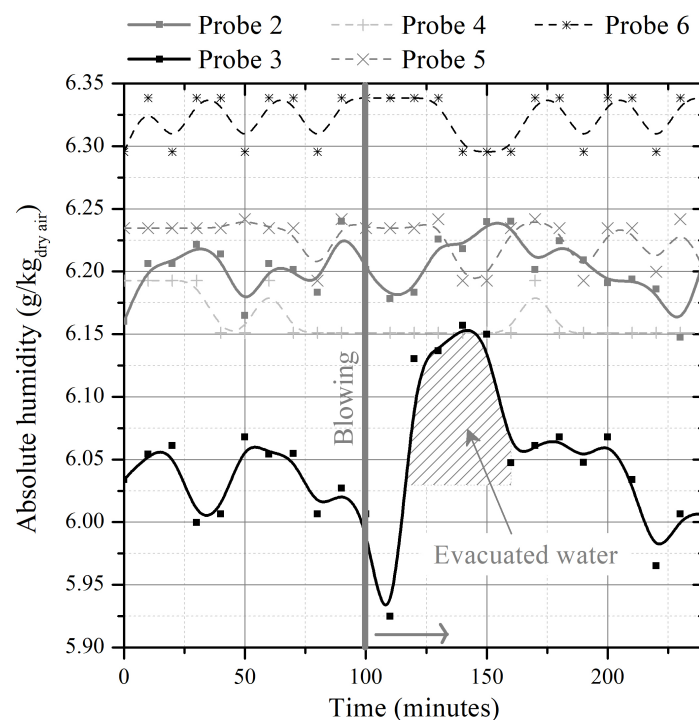


**Figure 14.** Evolution of absolute humidity in the wet wall during ventilation of the air space.

### 3.3. Approach of the Health Sustainability: Mould Growth and Development

The prediction of the development of biological activity cannot be carried-out with a single absolute humidity threshold. A number of studies have been carried out to propose biological activity models that are, for the moment, deterministic. Models such as the IEA Annex 14 [29], the Time-Of-Wetness model (TOW) [30] or the Johansson model [31] are based on relatively simple predictive parameters, while VTT models [32,33], isoproliferation (Ayerst [34], Smith et Hill [35], Clarke et Rowan [36], Hens [37], etc.) or bio-hygrothermal [38] models are more advanced deterministic models. All of these models still involve weaknesses, predict physically unrealistic phenomena, and/or show contradictions [39]. However, Johansson's model was chosen here because of its independent development of the nature of mold and its extensive testing campaign on facades with different thermal inertia, colors and orientations. Johansson studied the formulation of three indicators of mold growth: the first takes into account only the influence of relative humidity. The second adds a temperature-dependent element. Finally, the third indicator shows a function reflecting the delay in the growth of biological activity under unfavorable conditions. The Johansson indicator is defined as follows [31]:

$$I_3 = \frac{\int_{\tau=t_0}^{t_1} f_r(\tau)f_T(\tau)f_\phi(\tau)d\tau}{t_1 - t_0} \quad (7)$$

with  $f_T$  and  $f_\phi$  being two functions that are dependent on temperature and relative humidity, respectively. The function  $f_r$  takes the value 0 over the delay time  $t_r$  of the appearance of biological activity after unfavorable conditions, while the value 1 is assumed in all other cases. A recovery time ( $t_r$ ) of 24 h has been used herein [39]. Table 2 summarizes the results obtained for the three seasons investigated. Johansson's indicator shows low biological growth when ventilating the air gap during all three seasons with  $I_3$  values less than 1. On the other hand, data preceding the start-up of the ventilation system predict a higher bacteriological coverage area of up to 30% of the wall ( $I_3 = 2.9$ ). Thus, the ventilation device of the air space also seems to ensure the quality of the indoor air against the development of fungi and other moulds on the surface of damp walls.

**Table 2.** Coverage area obtained from Johansson's mould growth indice.

Ventilation Operating		$I_3$	Coverage Area
Summer	off	2.9	10% < Coverage < 30%
Summer	on	0.9	Coverage < 1%
Autumn	on	0.8	Coverage < 1%
Winter	on	0.5	No mould growth

#### 4. Conclusions and Perspectives

Signs of dampness through infiltration and capillary rise are major obstacles to energy renovation projects in old buildings. Several solutions are currently proposed on the renovation market. However, these solutions are generally expensive and not sustainable (decrease in efficiency over time, impacting the load-bearing structure). Hence, this paper describes and validates a system that creates an appropriately designed ventilated air gap between the wet walls and the thermal insulation of buildings in order to maintain the hygroscopic balance of the wall and to prevent water transfers to the insulation. This system involves both blowing and suction systems to mechanically ventilate the aforementioned air gap.

As a first step, an aeraulic dimensioning methodology was developed and validated. The general principles, calculations in series and in parallel of the intake and discharge flow rates, considering the linear and dynamic aeraulic pressure losses, have been validated by an experimental approach. The system was then implemented on a pilot site. This in situ experimental work allowed us to observe the superficial drying of the wet wall on a large scale. The absence of surface condensation on the wet wall ensured that the thermal performance of the internal insulation was maintained. The mechanisms of interaction between relative humidity and temperature, particularly at the interface between the cold and humid wall and the ventilated air space, were found to govern the efficiency of the aeraulic process. Over a full year of measurements, the wet wall was maintained in hygroscopic balance, around 90% RH, guaranteeing the preservation of its mechanical performance, while the insulation layer was kept moisture-free. In addition, a model for predicting the appearance and development of biological activity has been proposed but is yet to be validated quantitatively.

Hence, results can allow us to state that the proposed system satisfies the four specific objectives formulated in the introduction of this paper. Moreover, with respect to the fourth objective, a capital expenditure or cost of about 250–300 euros and operative expenditure or annual operation costs of less than 20 euros (ventilation and consequent heating cost) per dwelling make the proposed solution economically attractive.

These preliminary results show the interest of deepening the investigations in order to optimize such a system (increase performance, improve control and ensure lower

installation and low maintenance costs). On the one hand, additional laboratory studies must be carried out to identify the main factors governing the effectiveness of the device while limiting the measurement inherent biases in on-site instrumentation. The conditions of temperature and relative humidity of the cellar were relatively favorable for water transfers due to the presence of the boiler. Moreover, the influence of various parameters, such as the physical–mechanical properties of the materials, the solar radiation on the wall and the rain, were not taken into account in this approach. On the other hand, a refined and extended modeling of the global unsteady behavior of the integral wall will allow a versatile design method to be set up for engineers and installers. This numerical model will be based on material data sets from an experimental analysis platform to study capillary rise in a laboratory and under a controlled environment. In order to make this ventilation system autonomous, some additional probes could automatically switch on the system when a pre-selected humidity threshold is reached. This development will guarantee the performance of the system and the optimization of the operating times.

**Author Contributions:** Conceptualization, G.P.; methodology, O.D.; validation, D.R.R.; formal analysis, G.P. and D.R.R.; investigation, G.P. and O.D.; writing—original draft preparation, G.P. and O.D.; writing—review and editing, D.R.R.; supervision, T.L.; project administration, G.P. All authors have read and agreed to the published version of the manuscript.

**Funding:** This research received no specific external funding.

**Institutional Review Board Statement:** Not applicable.

**Informed Consent Statement:** Not applicable.

**Acknowledgments:** The authors would like to thank Marc Noel, Aéraulec compagny, and the Hauts-de-France Region for its support during this project. The third author acknowledges the NSERC for its financial support via the Discovery grant and the Michel Trottier private donation to the t3e research group.

**Conflicts of Interest:** The authors certify that they have NO affiliations with or involvement in any organization or entity with any financial interest (such as honoraria; educational grants; participation in speakers' bureaus; membership, employment, consultancies, stock ownership, or other equity interest; and expert testimony or patent-licensing arrangements), or non-financial interest (such as personal or professional relationships, affiliations, knowledge or beliefs) in the subject matter or materials discussed in this manuscript. The granting bodies had no role in the design of the study; in the collection, analyses, or interpretation of data; in the writing of the manuscript, or in the decision to publish the results.

## Nomenclature

### Greek

$\lambda$	head loss coefficient
$\rho$	air density, kg/m <sup>3</sup>
$\varphi$	relative humidity, %
$\varphi^{abs}$	absolute humidity, g/kg <sub>dry air</sub>

### Roman

$D$	segment inner diameter, m
$D_b$	sweep time, s
$L$	segments length, m
$M$	molar mass, g/mol
$P$	pressure, Pa
$P_v$	vapor partial pressure, Pa
$P_v^{sat}$	vapor saturation pressure, Pa
$P_s$	static pressure, Pa
$P_t$	operating point
$Q$	volumetric air flow rate, m <sup>3</sup> /s
$T$	temperature, K
$V$	mean air velocity, m/s

## Subscripts

<i>a</i>	air
<i>i</i>	indoor
<i>m</i>	wall
<i>s</i>	surface
<i>w</i>	water

## References

- Johansson, P.; Ekstrand-Tobin, A.; Svensson, T.; Bok, G. Laboratory study to determine the critical moisture level for mould growth on building materials. *Int. Biodeterior. Biodegrad.* **2012**, *73*, 23–32. [CrossRef]
- Udawattha, C.; Galkanda, H.; Ariyaratne, I.S.; Jayasinghe, G.; Halwatura, R. Mold growth and moss growth on tropical walls. *Build. Environ.* **2018**, *137*, 268–279. [CrossRef]
- Yu, S.; Yu, Z.; Liu, P.; Feng, G. Influence of environmental factors on wall mold in underground buildings in Shenyang City, China. *Sustain. Cities Soc.* **2019**, *46*, 101452. [CrossRef]
- Cony Renaud Salis, L.; Abadie, M.; Wargocki, P.; Rode, C. Towards the definition of indicators for assessment of indoor air quality and energy performance in low-energy residential buildings. *Energy Build.* **2017**, *152*, 492–502. [CrossRef]
- D'Ayala, D.; Aktas, Y.D. Moisture dynamics in the masonry fabric of historic buildings subjected to wind-driven rain and flooding. *Build. Environ.* **2016**, *104*, 208–220. [CrossRef]
- You, S.; Li, W.; Ye, T.; Hu, F.; Zheng, W. Study on moisture condensation on the interior surface of buildings in high humidity climate. *Build. Environ.* **2017**, *125*, 39–48. [CrossRef]
- Annala, P.J.; Hellemaa, M.; Pakkala, T.A.; Lahdensivu, J.; Suonketo, J.; Pentti, M. Extent of moisture and mould damage in structures of public buildings. *Case Stud. Constr. Mater.* **2017**, *6*, 103–108. [CrossRef]
- Annala, P.J.; Lahdensivu, J.; Suonketo, J.; Pentti, M.; Vinha, J. Need to repair moisture- and mould damage in different structures in finnish public buildings. *J. Build. Eng.* **2018**, *16*, 72–78. [CrossRef]
- ANSES. Moisissures Dans le Bâti. 2016. Available online: <https://www.anses.fr/fr/system/files/AIR2014SA0016Ra.pdf> (accessed on 30 March 2020).
- Kim, K.H.; Jahan, S.A.; Kabir, E. A review on human health perspective of air pollution with respect to allergies and asthma. *Environ. Int.* **2013**, *59*, 41–52. [CrossRef] [PubMed]
- Lee, H.; Ozaki, A.; Lee, M.; Cho, W. A fundamental study of intelligent building envelope systems capable of passive dehumidification and solar heat collection utilizing renewable energy. *Energy Build.* **2019**, *195*, 139–148. [CrossRef]
- Li, B.; Hua, L.; Tu, Y.; Wang, R. A Full-Solid-State Humidity Pump for Localized Humidity Control. *Joule* **2019**, *3*, 1427–1436. [CrossRef]
- Kreiger, B.K.; Srubar, W.V. Moisture buffering in buildings: A review of experimental and numerical methods. *Energy Build.* **2019**, *202*, 109394. [CrossRef]
- Lubelli, B.; van Hees, R.P.; Bolhuis, J. Effectiveness of methods against rising damp in buildings: Results from the EMERISDA project. *J. Cult. Herit.* **2018**, *31*, S15–S22. [CrossRef]
- de Freitas, V.P. *Humidade Ascensional*, FEUP ed.; Faculdade de Engenharia da Universidade do Porto: Porto, Portugal, 2008; Volume 3, ISBN 9789727521012
- af Klintberg, T.; Björk, F. Air Gap Method: Dependence of water removal on RH in room and height of floor air gap. *Build. Environ.* **2012**, *56*, 1–7. [CrossRef]
- af Klintberg, T.; Björk, F. Air Gap Method: Drying of a concrete slab on ground construction. *Struct. Surv.* **2010**, *28*, 281–299. [CrossRef]
- af Klintberg, T.; Björk, F. Air Gap Method: Measurements of airflow inside air gaps of walls. *Struct. Surv.* **2008**, *26*, 343–363. [CrossRef]
- af Klintberg, T.; Johannesson, G.; Björk, F. Air gaps in building construction avoiding dampness and mould. *Struct. Surv.* **2008**, *26*, 242–255. [CrossRef]
- Delgado, J.M.P.Q.; Guimarães, A.S.; de Freitas, V.P. *Air Drying Technologies Applied to Buildings Treatment*; Springer: Cham, Switzerland, 2014; pp. 1–26.
- Guimarães, A.S.; de Freitas, V.P. Wall base ventilation system as a new technique to treat rising damp in existent buildings. *J. Build. Apprais.* **2009**, *5*, 187–195. [CrossRef]
- Guimarães, A.S.; Delgado, J.M.P.Q.; de Freitas, V.P. Rising damp in building walls: The wall base ventilation system. *Heat Mass Transf.* **2012**, *48*, 2079–2085. [CrossRef]
- Guimarães, A.S.; Delgado, J.M.; de Freitas, V.P. Treatment of rising damp in historic buildings: Experimental campaign of wall base ventilation and interface effect analysis. *J. Cult. Herit.* **2016**, *20*, 733–738. [CrossRef]
- Torres, M.I.M.; Peixoto de Freitas, V. Treatment of rising damp in historical buildings: Wall base ventilation. *Build. Environ.* **2007**, *42*, 424–435. [CrossRef]
- Torres, I.; de Freitas, V.P. The influence of the thickness of the walls and their properties on the treatment of rising damp in historic buildings. *Constr. Build. Mater.* **2010**, *24*, 1331–1339. [CrossRef]

26. Kantoush, S.A.; Schleiss, A.J.; Sumi, T.; Murasaki, M. LSPIV implementation for environmental flow in various laboratory and field cases. *J. Hydro-Environ. Res.* **2011**, *5*, 263–276. [[CrossRef](#)]
27. Gornicki, K.; Winiczenko, R.; Kaleta, A.; Choinska, A. Evaluation of models for the dew point temperature determination. *Tech. Sci.* **2017**, *20*, 241–257. [[CrossRef](#)]
28. Rahim, M.; Douzane, O.; Tran Le, A.; Promis, G.; Langlet, T. Characterization and comparison of hygric properties of rape straw concrete and hemp concrete. *Constr. Build. Mater.* **2016**, *102*, 679–687. [[CrossRef](#)]
29. Hens, H. IEA Annexe 14. Condensation and energy. *J. Build. Phys.* **1992**, *15*, 261–273. [[CrossRef](#)]
30. Adan, O. On the Fungal Defacement of Interior Finished. Ph.D. Thesis, Eindhoven University of Technology, Eindhoven, The Netherlands, 1994.
31. Johansson, S.; Wadso, L.; Sandin, K. Estimation of mould growth levels on rendered façades on surface relative humidity and surface temperature measurements. *Build. Environ.* **2010**, *45*, 1153–1160. [[CrossRef](#)]
32. Hukka, A.; Viitanen, H. A mathematical model of mould growth on wooden materials. *Wood Sci. Technol.* **1999**, *33*, 475–485. [[CrossRef](#)]
33. Ojanen, T.; Peuhkuri, R.; Viitanen, H.; Lahdesmaki, K.; Vinha, J.; Salminen, K. Classification of materials sensitivity—New approach for mould growth modeling. In Proceedings of the 9th Nordic Symposium on Building Physics, Tampere, Finland, 29 May–2 June 2011; Volume 2, pp. 867–874.
34. Ayerst, G. The effects of moisture and temperature on growth and spore germination in some fungi. *J. Stored Prod. Res.* **1969**, *5*, 127–141. [[CrossRef](#)]
35. Smith, S.; Hill, S. Influence of temperature and water activity on germination and growth of *Aspergillus restrictus* and *A. versicolor*. *Trans. Br. Mycol. Soc.* **1982**, *79*, 558–560. [[CrossRef](#)]
36. Clarke, J.; Johnstone, C.; Kelly, N.; McLean, R.; Anderson, J.; Rowan, N.; Smith, J. A technique for the prediction of the conditions leading to mould growth in buildings. *Build. Environ.* **1999**, *34*, 515–521. [[CrossRef](#)]
37. Hens, H. Fungal Defacement in Buildings: A Performance Related Approach. *HVAC&R Res.* **1999**, *5*, 265–280.
38. Wufi. 2005. Available online: [www.hoki.ibp.fhg.de/wufi/downloads\\_e.html](http://www.hoki.ibp.fhg.de/wufi/downloads_e.html) (accessed on 25 April 2019).
39. Vereecken, E.; Roels, S. Review of mould prediction models and their influence on mould risk evaluation. *Build. Environ.* **2012**, *51*, 296–310. [[CrossRef](#)]